Catalysis Today xxx (xxxx) xxx-xxx

Contents lists available at ScienceDirect

Catalysis Today

journal homepage: http://ees.elsevier.com

Biocatalytic synthesis of poly[ε-caprolactone-*co*-(12-hydroxystearate)] copolymer for sorafenib nanoformulation useful in drug delivery

Izolda Kántor [a,c], Diana Aparaschivei [b], Anamaria Todea [b], Emese Biró [a,*], György Babos [a,c], Dóra Szerényi [c], Balázs Kakasi [c], Francisc Péter [b,*], Eugen Şişu [d], Tivadar Feczkó [a,c]

[a] *Institute of Materials and Environmental Chemistry, Research Centre for Natural Sciences, Magyar tudósok körútja 2, H-1117, Budapest, Hungary*
[b] *University Politehnica of Timişoara, Faculty of Industrial Chemistry and Environmental Engineering, Carol Telbisz 6, 300001, Timişoara, Romania*
[c] *Research Institute of Biomolecular and Chemical Engineering, University of Pannonia, Egyetem u. 10, H-8200, Veszprém, Hungary*
[d] *"Victor Babes" University of Medicine and Pharmacy Timisoara, 2 Eftimie Murgu Sq., 300041, Timişoara, Romania*

ARTICLE INFO

Keywords
poly[ε-caprolactone-co-(12-hydroxystearate)]
biocatalysis
hydrolases
sorafenib
nanoparticles
drug delivery

ABSTRACT

Nanoformulations can play an important role in the improvement of anticancer drug therapies. The bioavailability of sorafenib, which is the exclusively applied drug in the treatment of unresectable hepatocellular carcinoma, may be increased by its incorporation in a biocompatible nanoparticulate matrix that is capable of targeting and controlling the drug release. The copolymers of ε-caprolactone are emerging biodegradable compounds for drug delivery applications. In this work, an immobilized lipase and three native hydrolases, a lipase, an esterase and a protease (two of them not previously used as polyesterification catalysts) have been studied as biocatalysts for the synthesis of oligomers of ε-caprolactone and 12-hydroxystearic acid, proving different selectivity regarding the polymerization degree, ratio of linear and cyclic oligomers, and insertion of the fatty acid units in the polymeric chain. The synthesized poly[ε-caprolactone-*co*-(12-hydroxystearate)] was used as a novel encapsulating copolymer for preparation of sorafenib-loaded polymeric nanocomposites. The nanoparticle formulation by emulsion-solvent evaporation method was optimized for particle size and encapsulation efficiency. The developed nanotherapeutics showed promising drug release profile and cytotoxic effect *in vitro* in HepG2 hepatocellular cells.

1. Introduction

Hepatocellular carcinoma (HCC) is a life-threatening disease and, according to global cancer statistics from 2012, the second leading cause of cancer-related deaths in men and the sixth in women, worldwide [1]. Sorafenib is an anti-angiogenic multikinase inhibitor with cytostatic effects. At present, sorafenib is the only drug which is capable to prolong the life of patients suffered from HCC. However, the non-specific uptake of the drug into healthy tissues leads to a high toxicity and a variety of critical side effects.

However, the pronounced lipophilicity of the drug molecule is responsible for poor bioavailability and distribution into healthy tissues [2], thus, resulting in a requirement of high doses to be administered. To overcome these drawbacks in current cancer therapy nanocarrier-based delivery of sorafenib and the controlled release of the compound have been approached.

Nanomedicine is one of the most growing fields of pharmaceutics. Synthetic copolymers are versatile and tunable devices for producing drug delivery systems such as nanoparticles, micelles, vesicular polymersomes, polyplexes, polymer-drug conjugates, and dendrimers [3].

Poly(ε-caprolactone) (PCL) is one of the biodegradable polyesters widely utilized in biomedical applications like tissue engineering (processed as films, mats, or scaffolds) and controlled drug delivery (processed as nanoparticles, microparticles, electro spun mats, or scaffolds). However, these applications are still restricted due to its high hydrophobicity, slow degradation rate and slow drug release properties. [4]. To overcome these drawbacks, various macromolecular architectures and compositions were proposed, including copolymers of ε-caprolactone (ECL) with various co-monomers [5], or grafted PCL copolymers [6]. Although the production of PCL and PCL copolymers is performed mainly by chemical catalysis, using catalysts as stannous octanoate [7], biocatalysis emerged as a valuable alternative in the last decades [8,9].

Lipases are by far the most important enzymes used for the synthesis of green polymers, particularly aliphatic polyesters, including PCL and copolymers of ECL [10,11]. However, other enzymes like cutinases also demonstrated selectivity for polyesterification reactions [12,13].

Hydroxy fatty acids are important bio-based compounds able to participate in various polymerization reactions, leading to estolides [14] or elastomers with copolymer structure [15]. Particularly, 12-hydroxystearic acid is easily available by hydrogenation of ricinoleic acid and can be considered a biobased raw material for various polymers.

Biocompatible polymeric nanoparticles are promising tools for controlling and/or targeting passively or actively the tumorous tissues [16]. Nanoparticulate drug delivery systems of PCL copolymers can be synthesized by various methods considering the properties of encapsulating polymer and the active

* Corresponding authors.
E-mail addresses: emese.biro@gmail.com (E. Biró); francisc.peter@upt.ro (F. Péter)

agent (e.g. solubility). Solvent-displacement or nanoprecipitation [17,18], (double) emulsification-solvent evaporation [19,20] and dialysis [21] methods are widely used for nanoparticle preparation using PCL.

Polymer composition, molecular weight, temperature and pH substantially affect the degradation rate of PCL-based nanotherapeutics [22]. PCL was approved by FDA, and studies show its biocompatibility and non-toxicity [23,24], however, regarding nanopharmaceuticals additional factors such as particle size, morphology and surface features (e.g. adsorption capacity) also play important role in the cytotoxicity, thus, it must be tested for each new formulation.

In some work sorafenib microencapsulation was achieved using polyethylene glycol-PCL copolymers prepared by polymerization [25,26]. Recently, structurally different hydroxy-fatty acids were copolymerized with ε-caprolactone using immobilized lipases, which resulted in lower molecular mass compared to the chemical catalysis [27]. In this work other hydrolases were investigated for improving the synthesis of poly[ε-caprolactone-*co*-(12-hydroxystearate)] (ECL-12HSA), to be used as nanoparticle-sized drug delivery carrier. The smaller polymers can be advantageous for drug delivery applications, since the long chain polymers generally provide extremely prolonged release, which extends through the expected lifetime of the nanomedicines.

In the current work the copolymer, synthesized biocatalytically from ε-caprolactone and 12-hydroxystearic acid co-substrate, was used as a novel carrier for entrapping sorafenib into polymeric nanoparticles. The biocatalytic pathway for the synthesis of ECL copolyesters with hydroxy fatty acids, reported in a previous paper [27] was further developed by investigating three native esterases, and an immobilized lipase from *Candida antarctica* B which could be a substitute of the largely used Novozyme 435. Emulsion-solvent evaporation method was optimized for nanoparticle size and encapsulation efficiency. Drug release test was performed under *in vitro* acidic environment modelling the microenvironment in tumors. Finally, *in vitro* cytotoxicity and cellular uptake studies were carried out with the sorfenib-loaded ECL-12HSA nanoparticles.

2. Experimental

2.1. Materials

ε-Caprolactone (ECL, ≥98%), 12-hydroxystearic acid (12HSA, 99%), trans-2-[3-(4-t-butyl-phenyl)-2-methyl-2-pro-penylidene]malononitrile (DCTB, ≥99%), sodium trifluoroacetate (NaTFA, 98 %), toluene (>99%) and tetrahydrofuran (99%) were acquired from Sigma Aldrich (St. Louis, MO, USA) and were used as purchased. Immobilized *Candida antarctica* lipase B on microporous ion exchange resin (GF-CalB-IM) was obtained from GenoFocus Inc. (Korea Republic), while native Alcalase was a product of Novo Nordisk (Denmark). Native lipase from *Pseudomonas stutzeri* and native Esterase AR "Amano" were generous gifts of Meito Sagyo Co. (Japan) and Amano Enzyme Inc. (Japan), respectively. Polyvinyl alcohol (PVA, Mw = 30,000–70,000 g/mol, 87–90% hydrolyzed), dichloromethane (DCM), acetone, glacial acetic acid, dimethyl sulfoxide (DMSO), 1-ethyl-3(3-dimethylaminopropyl) carbodiimide (EDC), N-hydroxy succinimide (NHS), sodium dodecyl sulphate (SDS), 3-(4,5-dimethylthiazol-2-yl)-2,5-diphenyltetrazolium bromide (MTT), and DMEM (high glucose) medium were obtained from Sigma Aldrich (St. Louis, MO, USA). Sorafenib (free base) was purchased from Active Biochem (Hong Kong, China). Cyanine 5 amine was produced by Lumiprobe GmBH (Hannover, Germany). Calcein AM was obtained from Thermo Fisher Scientific (Waltham, MA).

2.2. Biocatalytic synthesis of the ECL-12HSA polyester

The polymerization reactions were carried out in organic solvent (toluene). An Eppendorf Thermomixer Comfort heating shaker (Eppendorf, Hamburg, Germany) was used, at 1200 rpm mixing speed and equimolar ratio of monomers. To obtain a homogenous reaction mixture, 0.1 mmoles 12HSA were mixed with 0.1 mmoles ECL in 1 mL of toluene for 30 minutes at 75 °C, then different amounts of the selected enzyme were added (100 mg in the case of immobilized GF-CalB-IM lipase; 20 mg in the case of the native enzymes: Alcalase, *Ps. stutzeri* lipase, or Esterase AR). The protein content of the native biocatalysts was determined by the Bradford assay. As the protein content values were close (about 0,9 mg protein/mg biocatalyst), the same amount of biocatalyst (20 mg) was added in all experiments with native enzymes. The reactions were carried out for 24 h at 50 °C. At the end of the reaction, the mixture was centrifuged at 6,000 rpm (3,420 g) for 5 min (U-320R centrifuge, Boeco, Hamburg, Germany), then the toluene solution was removed with a pipette, and the solvent was evaporated in a vacuum oven at room temperature, yielding the product. ε-Caprolactone was completely converted after 24 h, while for the 12-hydroxystearic acid the conversion values exceeded 90%. The analysis was accomplished by GC-MS, as described previously [27].

2.3. MALDI TOF-MS analysis of the polymerization product

The formation of the different polymerization products was demonstrated by MALDI TOF-MS analysis using an UltrafleXextreme Bruker spectrometer with FlexControl and FlexAnalysis software packages for acquisition and processing of the data (BrukerDaltonics, Bremen, Germany). The acceleration voltage was 25 kV. The sample preparation and analysis were accomplished using DCTB as matrix and NaTFA as ionization agent [14]. The calculated molecular weights of the possible products were compared to the molecular weights found in the MS spectra, to identify the formed polymeric compounds. The number average molecular weight (M_n), weight average molecular weight (M_w), polydispersity ($Đ_M$) values, and the relative copolymer and homopolymer content of the products have been calculated as described elsewhere [28].

2.4. Preparation of nanocomposites

Sorafenib was encapsulated by oil-in-water emulsion-solvent evaporation method. The organic phase was composed of 0.2 mL of 1% (w/v) sorafenib in acetone, which was added to 20 - 40 mg encapsulating polymer dissolved in 1-2 mL of DCM. The water phase consisted of a 0.5 - 1% (w/v) PVA solution in MilliQ water. The ratio of o/w phase was varied between 1:2 and 1:4. Blank nanoparticles were prepared without adding the drug solution to the polymer in DCM. After the organic phase addition to the water phase, they were emulsified by sonication using a sonicator (Heat Systems Ultrasonics Inc. Sonicator Cell Disruptor Model W 220 F, USA) at an ultrasonication intensity level of 6, for 30 s. The organic solvents were evaporated by magnetic stirring for 3 h under atmospheric pressure at room temperature. The nanoparticles were centrifuged by Z216 MK microcentrifuge (Hermle Labortechnik, Wehingen, Germany) at 21,380 g for 20 min, washed thrice, and redispersed in MilliQ water or phosphate-buffered saline (PBS, pH 7.4).

2.5. Nanoparticle characterization

2.5.1. Size and morphology

The size distribution of the nanoparticles was measured by dynamic light scattering using a Zetasizer Nano ZS (Malvern Instruments, Malvern, UK). Intensity mean diameter and polydispersity index (PDI) were presented as characteristic feature of the nanocomposites.

The morphology was investigated after centrifuging and redispersing the nanoparticles in distilled water, dropping them onto a grid, and drying them under room temperature. Then, they were examined with a FEI Apreo scanning electron microscope (SEM, Thermofisher, Waltham MA, USA) at 20 kV.

2.5.2. Yield and encapsulation efficiency

The nanoparticle yield was determined after drying 0.5 mL of washed nanoparticle suspension by gravimetry. Nanoparticles from 0.5 mL of centrifuged nanosuspension were dissolved in 1 mL of DMSO to determine the encapsulation efficiency. The solution was diluted to be detectable in the linear calibration range (1-20 μg/mL). The absorbance of the solutions was measured spectrophotometrically (Biochrom 4060, Pharmacia LKB, Cambridge, UK) at

the absorbance maximum of sorafenib (271 nm) in DMSO. The encapsulation efficiency of the active agents was calculated as follows:

Encapsulation efficiency (%) = (mass of drug in nanocomposite/mass of total drug) × 100

2.5.3. In vitro drug release test

The *in vitro* drug release of the nanocomposite was examined in ammonium acetate buffer (pH 5.5) that models the acidic tumor microenvironment. 0.5 mL Washed suspension containing 16 mg nanocomposites was mixed with 4.5 mL of ammonium acetate buffer and incubated at 37 °C in 5 mL non-transparent Eppendorf tubes and shaken in a Hettich Benelux MKR-13 Thermomixer (Hettich Benelux Laboratory Equipment, Geldermalsen, Netherlands), for 3 days at 1000 rpm. Three parallel samples were investigated. Aliquots were taken at 0.5, 1, 2, 4, 6, 12 h and every 24 h, 0.5 mL from each sample were centrifuged (Z216 MK microcentrifuge, Hermle Labortechnik, Wehingen, Germany) for 30 min at 21,380 g, washed three times with 1 mL of MilliQ water, the pellet was dissolved in 1 mL of DMSO, and the drug concentration was measured spectrophotometrically as written in section 2.4.2.

2.6. Nanoparticle labelling for cell studies

1 mL of nanoparticle suspension (10 mg/mL) was centrifuged and washed with MilliQ water, resuspended in 1 mL of MilliQ water, then, 0.1 mL solution of EDC (10 mg) and NHS (10 mg) in MilliQ water was added and incubated for 60 min at 25 °C. After the nanoparticle activation, the suspension was centrifuged and washed with MilliQ water, and redispersed in 1 mL of MilliQ water. The obtained carbodiimide-activated nanoparticle dispersion was pipetted to a 100 μL of PBS (pH 7.4) solution containing 0.5 mg/mL Cyanine 5 amine fluorescent dye, and incubated for 1 h at 25 °C. Then, the nanocomposite dispersion was centrifuged, washed three times, and redispersed in 1 mL of PBS.

2.7. Cell cultures

The human cancer cell line HepG2 was grown in DMEM medium supplemented with 10% fetal calf serum (FCS) and 100 U/mL penicillin. The cells were cultured at 37 °C in a humidified atmosphere containing 5% CO_2. They were trypsinized, resuspended, and precultured before use.

2.8. Cytotoxicity and in vitro cellular uptake studies

In vitro cytotoxicity in HepG2 cells was analyzed using MTT reagent. Cells were seeded (10^5 cells/well) in 96-well plates. After 24 h of pre-incubation, 100 μL of fresh DMEM medium containing 10% FCS was added to the growth media. After another 24 h incubation, the media was changed with 200 μL of fresh DMEM containing the drug-loaded nanoparticles. Three different sorafenib concentration levels of the added nanocomposites were applied: 2.5, 5.0, 12.5 and 25.0 μg/mL. After 24 h of incubation, 100 μL of fresh DMEM medium was added, then the incubation continued for another 24 h. 20 μL/well of MTT solution (5 mg MTT/mL) and 200 μL/well supplemented culture media were added followed by further incubation for 2 h. The supernatant was removed, and the cells were lysed by MTT lysis solution (DMSO, 1% acetic acid, 10% SDS). The absorbance was measured at 490 nm by a VictorX3 plate reader (Perkin Elmer, Waltham, MA, USA). The percentage of viable cells was calculated by relating it to the negative control (untreated cells). The data were presented as the mean and standard deviation with eight replicates.

Flow cytometry was used to examine nanoparticle uptake by HepG2 cells. The cells were cultured in 24-well plates at a cell density of 2×10^5 cells/well at 37 °C for 24 h. After cultivation, 100 μg of fluorescently labelled nanoparticles were added to each of the wells and incubated for 24 h. Cells without nanoparticle addition were used as a negative control. The cells were washed by PBS, trypsinized, and resuspended in PBS containing 2% BSA. The living cells were stained by Calcein AM. Flow cytometry was performed on a Gallios Flow Cytometer (Beckman Coulter, Brea, CA, USA) at Ex/Em wavelengths of 488/525 nm for Calcein AM and 633/660 nm for Cyanine 5. Every sample was analyzed in triplicate.

3. Results and Discussion

3.1. Synthesis of poly[ε-caprolactone-co-(12-hydroxystearate)] catalyzed by esterases

Three native hydrolases and one immobilized lipase were used as biocatalysts for the polymerization of 12HSA and ECL, in organic reaction medium. The synthesis of oligoesters starting from these monomers was already accomplished in our group, by both chemical and enzymatic route [27,29], but for this study different biocatalysts were tested, for possible improvement of catalytic efficiency and selectivity. The polyesterification products which can be formed in these reactions are depicted in Fig. 1. Branched linear and cyclic copolymers containing a random distribution of 12HSA and ECL monomer units were synthesized, along with linear and cyclic homopolymers as secondary products.

The formation of the copolyesters was demonstrated based on MALDI-TOF MS spectra. An example of MALDI TOF-MS spectrum is presented in Fig. S1 (Supplementary Material). The main products that can be formed are linear and cyclic copolymers containing 12HSA units inserted in the PCL back-

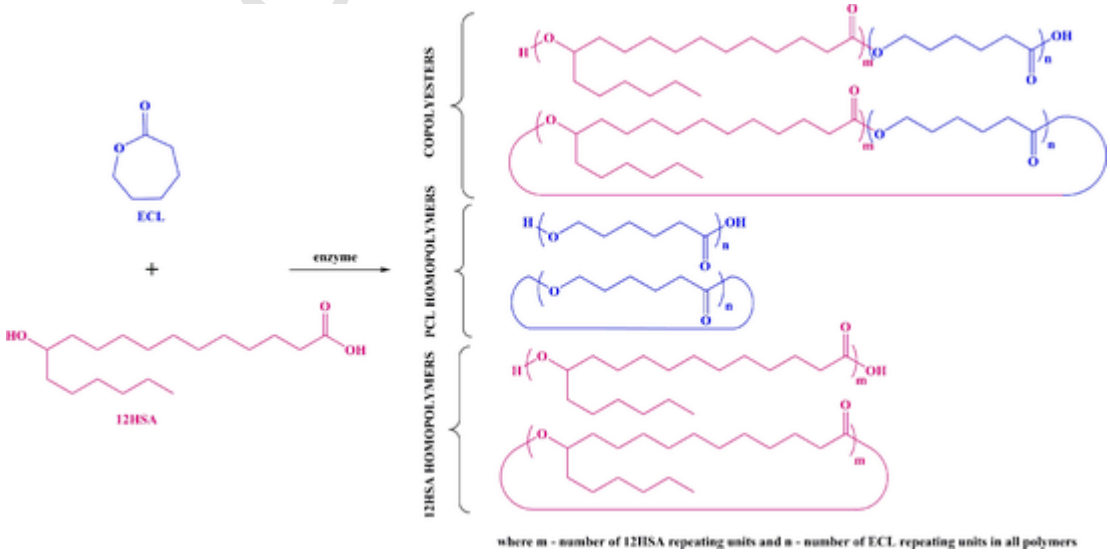

Fig. 1. Reaction scheme of the synthesis of copolyesters and homopolyesters from ε-caprolactone and 12-hydroxystearic acid.

bone, alongside linear and cyclic homopolymers of 12HSA and ECL as byproducts. The highlighted peak values, with m/z 666.2, 780.3 and 894.5 Da, correspond to the Na^+ adducts of linear copolyesters $(12HSA)_1$-$(ECL)_{3-5}$. Another series identified in the MALDI TOF-MS spectrum were the cyclic copolyesters $(12HSA)_2$-$(ECL)_{1-3}$, with the peak values (highlighted in Fig. S1) at m/z 702.3, 816.5 and 930.7 Da. Homopolymers were also found, e.g. the peak value with m/z 752.2 Da corresponds to the Na^+ adducts of linear homopolymers containing six ECL units.

The relative compositions of the polymerization products, synthesized at equimolar ratio of 12HSA and ECL monomers, were calculated from the MALDI-TOF MS analysis data and are presented in Table 1.

The immobilized lipase GF-CalB-IM was less efficient compared with Novozyme 435, used in a previous study, when an average molecular weight of about 1400 and maximal polymerization degree of 14 were achieved [27]. Obviously, this lipase is not specific for the polymerization of ECL and 12HSA, although it was the most efficient biocatalyst for other polymerization reactions of ECL, with 5-hydroxymethyl-2-furancarboxylic acid [30].

As shown in Table 1, all three native hydrolases (a lipase, an esterase and a protease) proved to be efficient for the synthesis of the ECL-12HSA copolymer, but the specificity and catalytic efficiency were highly dependent on the nature of the enzyme. The highest copolymer content in the polymerization product was obtained using Esterase AR "Amano" as biocatalyst, but the average molecular weight was lower compared to the other hydrolases and only one hydroxy-fatty acid unit was found in the copolymer backbone in all identified polymerization products. Probably, the reaction starts by the formation of the monoester of 12HSA and ECL, but the further chain growth is accomplished only by ring-opening polymerization of ECL, due to the higher specificity of the enzyme for this monomer. Although 12HSA is included in the poly(ε-caprolactone) chain as a single terminal unit, these compounds could be also interesting for biomedical applications, considering the different shape and hydrophobicity compared to the PCL homopolymers.

Using Alcalase, the highest average molecular weight of 1850 Da and a maximal polymerization degree of 17 were obtained, while the relative content of PCL homopolymer did not exceed 30%. Even if proteases are not known as polycondensation catalysts, they were successfully used for the oligomerization of alkyl L-lactates, but Alcalase (immobilized as CLEA) was not active in these reactions [31]. Therefore, these results are very promising, and new tailor-made immobilized biocatalysts will be developed in the future studies.

Relative copolymer content higher than 85% and polymerization degree of 8 were obtained when the native *Ps. stutzeri* lipase has been used as biocatalyst. Although the number average molecular weights (M_n) did not exceed 900 Da, they were comparable with those reported for another native lipase, from *Pseudomonas fluorescens* [27], but with different linear/cyclic copolymer selectivity. This enzyme yielded the highest cyclic copolymer content and such a selectivity could be equally interesting for future developments, considering that cyclic polyesters present particular interest since their biodistribution varies from their linear analogs [32].

The most important outcome of this study is that besides lipase other esterases can be also successfully employed for the synthesis of ECL-12HSA copolymers, leading to specific characteristics of these products in terms of average molecular mass, structure of the copolymer, linear/cyclic copolymer ratio. The copolymer synthesized by Alcalase was selected for the nanoparticle formulation study based on its higher molecular weight, but all these materials could have promising applications.

3.2. Physical and chemical features of nanoparticles

It is known from previous results [33] that higher molecular weight results in slower drug release and higher encapsulation efficiency, hence, we used the copolymer with the highest molecular weight for nanoparticle preparation. The synthesized copolymer of (ECL-12HSA) was utilized to encapsulate sorafenib anticancer agent using oil-in-water emulsion-solvent evaporation technique. For the optimization of the method, the effect of most important process parameters such as emulsifier concentration, ratio of oil and water phases as well as initial drug and polymer concentration were investigated on the size and drug encapsulation efficiency. 0.5% or 0.75% (w/v) PVA concentration was found to be too low for the emulsification, since they resulted in too high (>0.2) PDI indicating aggregation or the precipitation of a portion of the drug separately from the nanocomposites (Fig. 2). However, with 1% (w/v) PVA in the water phase, choosing suitable encapsulating polymer and sorafenib concentration provided monodisperse size distribution with PDI < 0.2 (Table 2). Oil/water ratio 1:2 was optimal at the applied sonication energy, since at higher ratio (1:4) the particle yield became much lower (<50%) related to 74 ± 4.0% obtained for 1:2. The low yield generally accompanies with lower encapsulation efficiency. Thus, the concentrations of encapsulating polymer and sorafenib were optimized using 1% PVA and 1:2 oil/water ratio. Increasing the copolymer concentration from 10 mg/mL to 20 mg/mL in the organic phase enhanced the size of the nanoparticles, although the PDI still remained suitably low (Table 2).

Interestingly, the polymer concentration also influenced the zeta potential of nanoparticles; the nanoparticles prepared by lower polymer amount had higher zeta potential (10 mg/mL: -18.1 ± 2.9 mV, 20 mg/mL: -9.2 ± 1.3 mV) suggesting higher stability, which can be the result of higher sorafenib amount on the surface of nanoparticles formed with less encapsulating polymer. Nevertheless, it must be noted that PVA emulsifier as a steric stabilizer might have higher stabilizing effect that cannot be measured by zeta potential analysis.

The sorafenib concentration is investigated in relation with the matrix polymer concentration, because the appropriate ratio of hydrophobic drug and incorporating polymer can give a homogenously dispersed mixture in the nanocomposite. The enhancement of drug concentration (related to the polymer concentration) from 5% to 10% did not cause significant change in size, nevertheless at 20%, the PDI increased substantially (Table 3) indicating the precipitation of drug outside of the nanocomposites as observed also in the size distribution (Fig. 3).

Increasing the sorafenib-to-copolymer ratio from 5% to 10% did not result in significantly different encapsulation efficiency, while further increase to 20% raised it substantially, though, the latter initial amount of sorafenib resulted in separately precipitated or aggregated nanoparticles (see in Fig. 3), which is undesirable and also determined as encapsulated drug, since this fraction is not separated from the submicron-sized particles during measurement of drug content.

Table 1
Influence of the biocatalyst on the average molecular weights and composition of the copolymerization products (calculated from MALDI-TOF MS data). Reaction conditions: 50 °C, equimolar monomer concentrations, 24 h reaction time, 1200 rpm mixing speed.

Enzyme	M_n [Da]	M_w [Da]	$Đ_M$	Composition of the product [%]						DP_{max}
				LC	CC	LHE	LHH	CHE	CHH	
GF-CalB-IM lipase	689	692	1.00	26.2	41.6	10.3	0.0	21.9	0.0	5
Ps. stutzeri lipase	854	911	1.07	39.1	49.4	0.7	7.7	1.6	1.5	8
Esterase AR	726	730	1.01	> 99.0	n.d.	n.d.	n.d	n.d.	n.d	5
Alcalase	1750	1850	1.06	68.3	3.4	11.9	4.3	8.7	3.4	17

LC - linear copolymer; CC - cyclic copolymer; LHE - linear homopolymer of ECL; LHH - linear homopolymer of 12HSA; CHE - cyclic homopolymer of ECL; CHH - cyclic homopolymer of

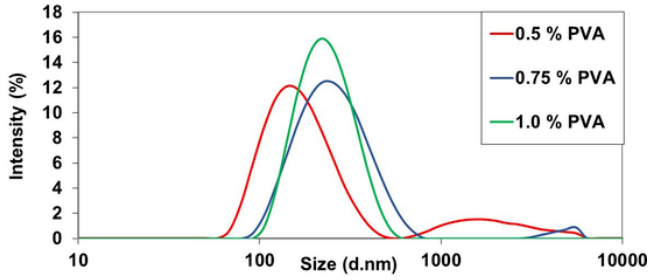

Fig. 2. Size distribution of sorafenib-loaded ECL-12HSA nanoparticles as a function of PVA emulsifier concentration.

Table 2
Influence of polymer concentration on the size of nanocomposites.

Polymer concentration (mg/mL)	Mean size by intensity (nm)	PDI
10	223 ± 7.1	0.175 ± 0.024
20	254 ± 16.1	0.177 ± 0.012

Table 3
Size of sorafenib-loaded ECL-12HSA nanoparticles as a function of initial drug concentration (%) related to copolymer concentration.

Sorafenib concentration (%)	5	10	20
Mean size by intensity (nm)	228 ± 5.0	219 ± 5.2	241 ± 3.2
PDI	0.172 ± 0.019	0.168 ± 0.029	0.288 ± 0.018

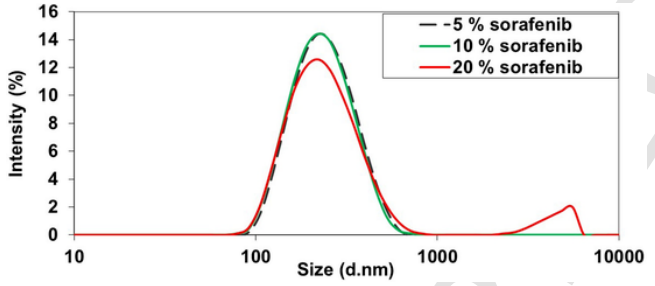

Fig. 3. Size distribution of nanocomposites at various sorafenib concentration related to initial encapsulating copolymer amount.

SEM showed much smaller size of nanoparticles (Fig. 4) than the dynamic light scattering method, since the latter one provides hydrodynamic size that is generally larger than the dry size. The nanoparticles had spherical shape as expected.

Overall, the optimal processing parameters for manufacture of sorafenib-loaded ECL-12HSA nanoparticles were 1% (w/v) PVA in the water phase, 2:1 water/oil ratio, 10 mg/mL encapsulating polymer concentration in the organic phase and 10% drug amount in relation with the initial polymer amount. For the drug release and cellular studies, the nanocomposites were formulated using these conditions.

3.3. In vitro drug release

The sorafenib release of the optimized nanoparticles was tested in acidic buffer (pH 5.5) mimicking the tumorous environment. The initial burst of drug was 62 ± 4.3%, then, a sustained active agent liberation occurred, while 79 ± 12.3% of the total amount was released during the 72 h study (Fig. 5). The relatively high fluctuation of the results may suggest drug adsorption in some phase of the degradation of the polymer matrix.

3.4. Cytotoxicity and cellular uptake of nanoparticles

In vitro MTT cytotoxicity assay was performed with an HCC cell line in order to examine the efficacy of the drug loaded nanoparticles against HepG2 cells. The nanoparticles showed concentration-dependent cytotoxicity (Fig. 6), and the nanocomposites with highest drug concentration (25 μg/mL in the cell medium) showed similar toxicity (33.2 ± 5.7% viability) as the pure drug (37.8 ± 2.4%) in the same cells, which latter value was published in our very recent work [34].

Cellular uptake of nanoparticles was also tested with the same cell line. The uptake of both drug loaded and blank nanoparticles was investigated. After 24 h incubation, 24.4 ± 8.4% of the living cells associated with the blank nanoparticles, while only 5.7 ± 1.6% of the sorafenib-loaded nanocomposites was connected to the cells. The significantly lower uptake of nanoparticles containing the medicine can be explained by the fact that the dead cells were not analyzed in the flow cytometry method, and through the 24 h duration of the test, substantial part of cells must have died. Although the blank nanoparticle uptake by the cells was also substantially lower than that suggested by the cytotoxicity results, consequently, probably the released drug took also substantial part in the elimination of the cancer cells.

4. Conclusions

Oligomers of ECL and 12HSA are exciting new compounds for biomedical applications. Alongside lipases, other hydrolases like Esterase AR "Amano" and Alcalase have been proved as efficient biocatalyst for this biocatalytic polymerization process. The nature of the enzyme influences the molecular mass, linear/cyclic selectivity and distribution of the monomeric units along the chain. By appropriate selection of the nature of the enzyme, the properties of the oligomeric biomaterial can be tailored in accordance to the specific requirements of the targeted application. The copolymer with the highest molecular weight was used for the formulation of the nanoparticles, as higher molecular weight leads to slower drug release and higher encapsulation efficiency but increasing the molecular weight above a certain limit results in too prolonged drug release, which is also not acceptable. Sorafenib anticancer drug was successfully entrapped by the biocatalytically synthesized ECL-12HSA copolymer. The emulsion-solvent evaporation method for the preparation of nanocomposites was optimized for size and encapsulation efficiency. The developed nanopharmaceuticals were very efficient against HepG2 HCC cells, and displayed promising sustained drug delivery *in vitro* in model tumor environment. Further studies will be carried out to correlate the structural characteristics of the synthesized copolymers with the encapsulation efficiency and drug-release profile of the nanocomposites, by appropriate tailoring of the biocatalyst selectivity (Table 4).

Author statement

All authors contributed to this research work, as follows: Izolda Kántor: investigation, original draft preparation; Diana Aparaschivei: investigation, resources; Anamaria Todea: conceptualization, methodology, writing-original draft; Emese Biró: methodology, validation, writing-original draft; György Babos: investigation, formal analysis; Dóra Szerényi: investigation; Balázs Kakasi: investigation; Francisc Peter: conceptualization, supervision, funding acquisition; writing-review & editing; Eugen Șișu: investigation, validation; Tivadar Feczkó: conceptualization, resources, funding acquisition, writing-review & editing.

Declaration of Competing Interest

The authors declare that they have no known competing financial interests or personal relationships that could have appeared to influence the work reported in this paper.

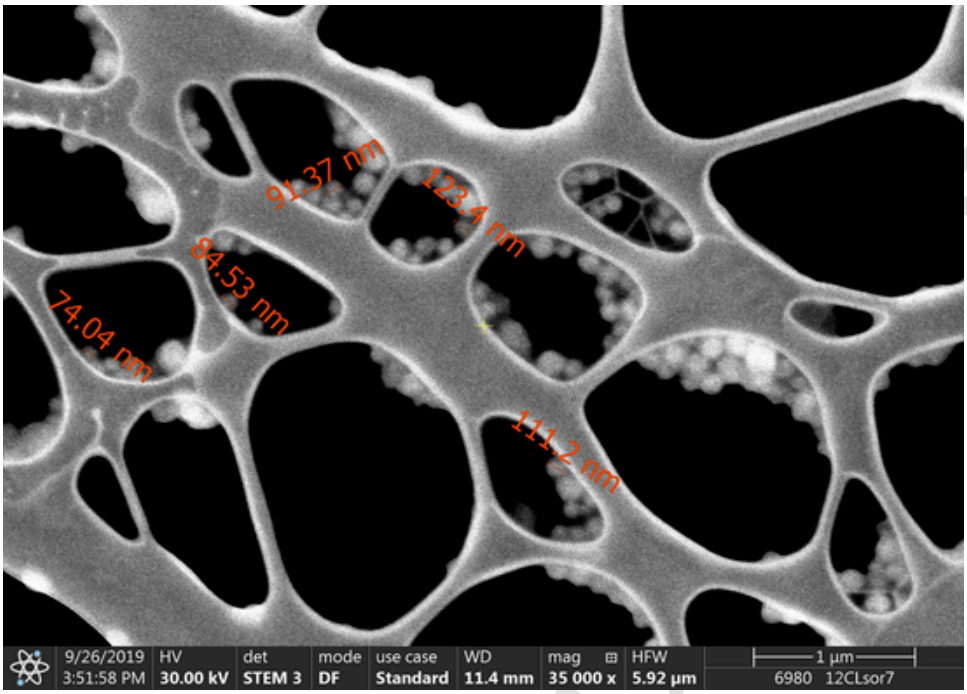

Fig. 4. SEM image of sorafenib-loaded ECL-12HSA nanoparticles on the metal grid.

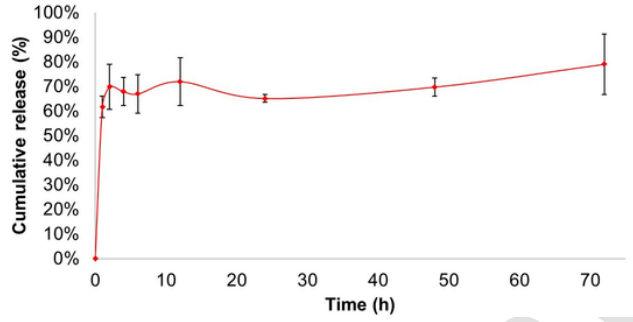

Fig. 5. Cumulative drug release from sorafenib-loaded ECL-12HSA nanoparticles in acetate buffer (pH = 5.5).

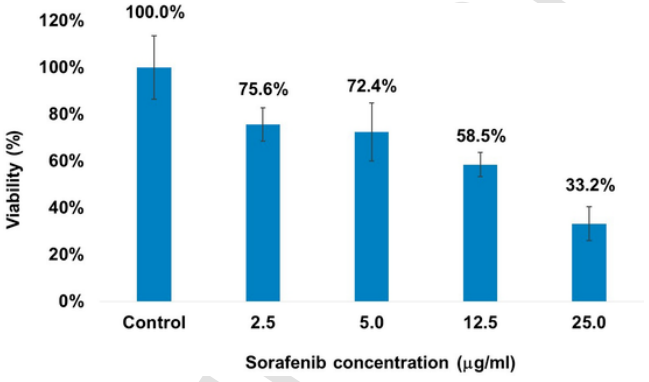

Fig. 6. Cytotoxicity of sorafenib-loaded ECL-12HSA nanocomposites with increasing drug concentration studied in HepG2 cells *in vitro*.

Table 4
Effect of initial sorafenib concentration (%, related to copolymer concentration) on the encapsulation efficiency of nanocomposites.

Sorafenib concentration (%)	5	10	20
Encapsulation efficiency (%)	61.5 ± 6.7	64.1 ± 8.5	72.7 ± 7.7

Acknowledgements

The authors acknowledge the generous donation of the Esterase AR "Amano" by Amano Enzyme Inc. (Japan), and *Pseudomonas stutzeri* lipase by Meito Sagyo Co. (Japan).

This work was supported by the grants provided by the National Competitiveness and Excellence Program, Hungary (NVKP_16-1-2016-0007) and by the BIO-NANO_GINOP-2.3.2-15-2016-00017 project. Dr. Tivadar Feczkó acknowledges the funding of Alexander von Humboldt Foundation (Ref. No.: 3.3-UNG/1161203 STP and 3.3-1161203-HUN-HFST-E) and the support of Hungarian Academy of Sciences via Bilateral Joint Project with the Polish Academy of Sciences. S/TEM studies were performed at the electron microscopy laboratory of the University of Pannonia, established using grant no. GINOP-2.3.3-15-2016-0009 from the European Structural and Investments Funds and the Hungarian Government. We are grateful to Ágnes Telbisz for providing the plate reader.

Appendix A. Supplementary data

Supplementary material related to this article can be found, in the online version, at doi:https://doi.org/10.1016/j.cattod.2020.05.005.

References

[1] L A Torre, F Bray, R L Siegel, J Ferlay, J Lortet-Tieulent, A Jemal, CA Cancer J. Clin. 65 (2015) 87–108.
[2] A Heidarinasab, H A Panahi, M Faramarzi, F Farjadian, Mater. Sci. Eng. C. 67 (2016) 42–50.
[3] M D Joshi, V Patravale, R Prabhu, Int. J. Nanomed. 10 (2015) 1001–1018.
[4] E Malikmammadov, T E Tanir, A Kiziltay, V Hasirci, N Hasirci, J. Biomat. Sci., Polym. Ed. 29 (2018) 863–893.
[5] C M Dong, K Y Qiu, Z W Gu, X De Feng, Macromolecules 34 (2001) 4691–4696.
[6] A Al Samad, A Bethry, E Koziolova, M Netopilık, T Etrych, Y Bakkour, J Coudane, F El Omar, B Nottelet, J. Mater. Chem. B 4 (2016) 6228–6239.
[7] M A Woodruff, D W Hutmacher, Prog. Polym. Sci. 35 (2010) 1217–1256.
[8] M Labet, W Thielemans, Chem. Soc. Rev. 38 (2009) 3484–3504.

[9] S Shoda, H Uyama, J Kadokawa, S Kimura, S Kobayashi, Chem. Rev. 116 (2016) 2307–2413.
[10] S Kobayashi, Polym. Adv. Technol. 26 (2015) 677–686.
[11] T Debuissy, E Pollet, L Avérous, ChemSusChem 11 (2018) 3836–3870.
[12] M Hunsen, A Azim, H Mang, S R Wallner, A Ronkvist, W Xie, R A Gross, Macromolecules 40 (2007) 148–150.
[13] V Ferrario, A Pellis, M Cespugli, G M Guebitz, L Gardossi, Catalysts 6 (2016) 205.
[14] A Todea, L G Otten, A E Frissen, I W C E Arends, F Peter, C G Boeriu, Pure Appl, Chem. 87 (2015) 51–58.
[15] H Ebata, K Toshima, S Matsumura, Macromol. Biosci. 8 (2008) 38–45.
[16] F Danhier, O Feron, V Preat, J. Control. Release 148 (2010) 135–146.
[17] H K Manjili, H Malvandi, M S Mousavi, E Attari, H Danafar, Artif. Cell. Nanomed. B. 46 (2018) 926–936.
[18] J P Abriata, R C Turatti, M T Luiz, G L Raspantini, L B Tofani, R L F do Amaral, K Swiech, P D Marcato, J M Marchetti, Mat. Sci. Eng. C-Mater. 96 (2019) 347–355.
[19] A T Alex, A Joseph, G Shavi, J V Rao, N Udupa, Drug Deliv 23 (2016) 2144–2153.
[20] R D Piazza, J V Brandt, G G Gobo, A C Tedesco, F L Primo, R F C Marques, M Jafelicci Jr., Colloid Surface A. 555 (2018) 142–149.
[21] W Y Ning, P Shang, J Wu, X Y Shi, S X Liu, Polymers-Basel 10 (2018) E214.
[22] P Grossen, D Witzigmann, S Sieber, J Huwyler, J Control, Release 260 (2017) 46–60.
[23] H Sun, L Mei, C Song, X Cui, P Wang, Biomaterials 27 (2006) 1735–1740.
[24] J-H Byun, H A R Lee, T H Kim, J H Lee, S H Oh, Biomater. Res. 18 (2014) 1.
[25] H Y Gan, L Z Chen, X M Sui, B Q Wu, S P Zou, A M Li, Y C Zhang, X K Liu, D L Wang, S Y Cai, X K Liu, Y Liang, X L Tang, Mat. Sci. Eng. C-Mater. 91 (2018) 395–403.
[26] X L Tang, Y G Lyu, D Xie, A M Li, Y Liang, D H Zheng, J Biomed, Nanotechnol. 14 (2018) 396–403.
[27] A Todea, D Aparaschivei, V Badea, C G Boeriu, F Peter, Biotechnol. J. 13 (2018) 1700629.
[28] A Todea, V Badea, L Nagy, S Kéki, C G Boeriu, F Peter, Acta Biochim. Pol. 61 (2014) 205–210.
[29] D Aparaschivei, A Todea, I Păușescu, V Badea, M Medeleanu, E Şişu, M Puiu, A Chiriță-Emandi, F Peter, Pure Appl. Chem. 88 (2016) 1191–1201.
[30] A Todea, I Bîtcan, D Aparaschivei, I Păușescu, V Badea, F Péter, V D Gherman, G Rusu, L Nagy, S Kéki, Polymers 11 (2019) 1402.
[31] H Ohara, E Nishioka, S Yamaguchi, F Kawai, S Kobayashi, Biomacromolecules 12 (2011) 3833–3837.
[32] J N Hoskins, S M Grayson, Macromolecules 42 (2009) 6406–6413.
[33] C Raman, C Berkland, K Kim, D W Pack, J Control, Release 103 (2005) 149–158.
[34] T Feczkó, A Piiper, T Pleli, C Schmithals, D Denk, S Hehlgans, F Rödel, T J Vogl, M G Wacker, Pharmaceutics 11 (2019) E489.